Supporting Information

Ion-selective Copper Hexacyanoferrate with Open-framework Structure Enables High-voltage Aqueous Mixed-ion Batteries

Ping Jiang[a,b,c], Hezhu Shao[a,c], Liang Chen[a,c]*, Jiwen Feng[b,c], Zhaoping Liu[a,c]*

[a] Key Laboratory for Graphene Technology and Application of Zhejiang Province, Ningbo Institute of materials Technology and Engineering, Chinese Academy of Sciences, Ningbo 315201, P.R. China
[b] Wuhan Institute of Physics and Mathematics, Chinese Academy of Sciences, Wuhan 430071, P.R. China
[c] University of Chinese Academy of Sciences, Beijing 100000, P.R. China

* Corresponding author. E-mail: cl@nimte.ac.cn, liuzp@nimte.ac.cn.

Figure S1.

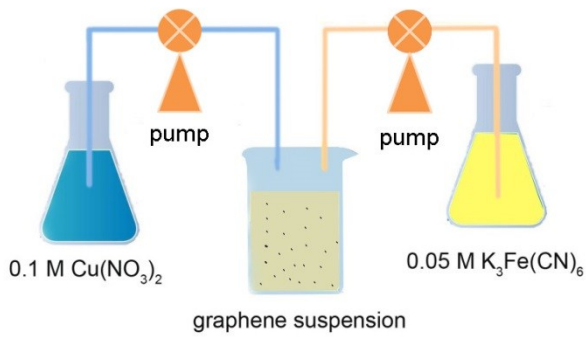

Figure S1. A scheme of the co-precipitation process for CuHCF/Gr.

Figure S2

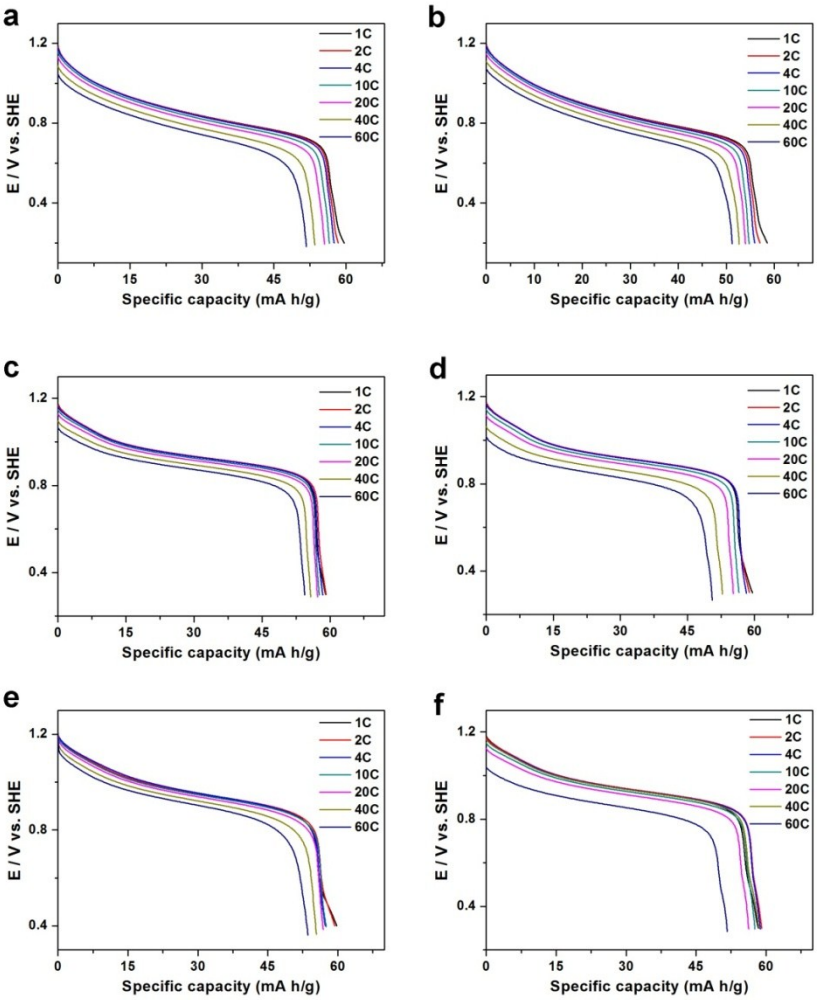

Figure S2. Rate capabilities of CuHCF in aqueous 0.1 M Li_2SO_4 + 0.4M Na_2SO_4 (**a**), 0.25 M Li_2SO_4 + 0.25 M Na_2SO_4 (**b**), 0.1 M Li_2SO_4 + 0.4M K_2SO_4 (**c**), 0.25 M Li_2SO_4 + 0.25 M Na_2SO_4 (**d**), 0.1 M Na_2SO_4 + 0.4 M K_2SO_4 (**e**), and 0.25 M Na_2SO_4 + 0.25 M K_2SO_4 (**f**). 1C equals to 60 mA g^{-1}.

Figure S3

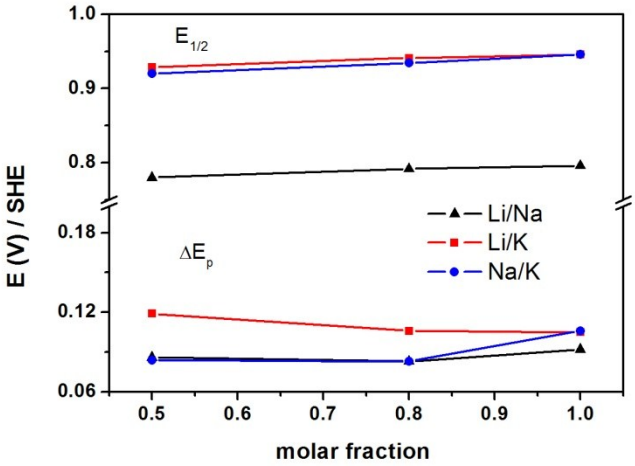

Figure S3. Plots of $E_{1/2}$ and ΔE_p vs. the mole fraction of Li^+/Na^+, Li^+/K^+, and Na^+/K^+ mixed-ion electrolytes. $E_{1/2}$, formal potential, the average of the anode and cathode peak potentials; ΔE_p, the difference voltage between anode and cathode peak potentials.

Figure S4

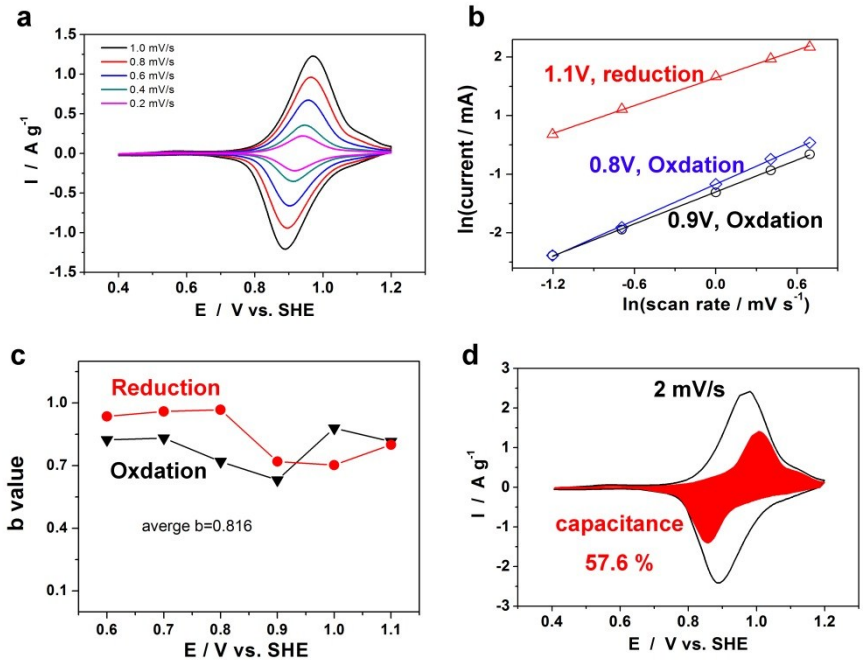

Figure S4. (a) Cyclic voltammograms of CuHCF/Gr in 0.4 M K_2SO_4 + 0.1 M Na_2SO_4 at various scan rates. (b) The fitted lines of ln(peak current) versus ln(scan rate) at different reduction/oxidation potentials. (c) *b*-value obtained at different reduction/oxidation potentials. (d) Cyclic voltammogram of CuHCF/Gr in 0.4 M K_2SO_4 + 0.1 M Na_2SO_4 at a scan rate of 2 mV s^{-1} with the capacitive contribution (the red region).

The currents (i) at various scan rates (v) should obey the power law (equation 1 and 2), where *a* and *b* are adjustable parameters.

$$i = av^b \tag{1}$$

$$Ini = bInv + Ina \tag{2}$$

For a redox reaction limited by semi-infinite diffusion, the peak current *i* varies as $v^{1/2}$ (b = 1); for a capacitive process, it varies as v (b = 0.5). The CV curves of CuHCF/Gr in 0.4 M K_2SO_4 + 0.1 M Na_2SO_4 electrolytes at various scan rates are recorded in Figure S4a. From the ln$i$ *vs.* ln$v$ curves in Figure S4b, the average b value is found to be 0.82, demonstrates that a combination of capacitive process and diffusion-limited redox reactions manages the electrochemical reaction. Thus, the i value consists of two parts, and can be expressed as following equation:

$$i = k_1 v + k_2 v^{1/2} \tag{3}$$

As k_1 and k_2 are always fixed for the same electrochemical reaction, we can calculate k_1 and k_2 through the equation 3. The capacitance contribution of CuHCF/Gr in 0.4 M K_2SO_4 + 0.1 M Na_2SO_4 is found to be 57.6%, which accounts for the high rate capability of CuHCF/Gr. Similar phenomenon are found in other electrolytes.

Figure S5

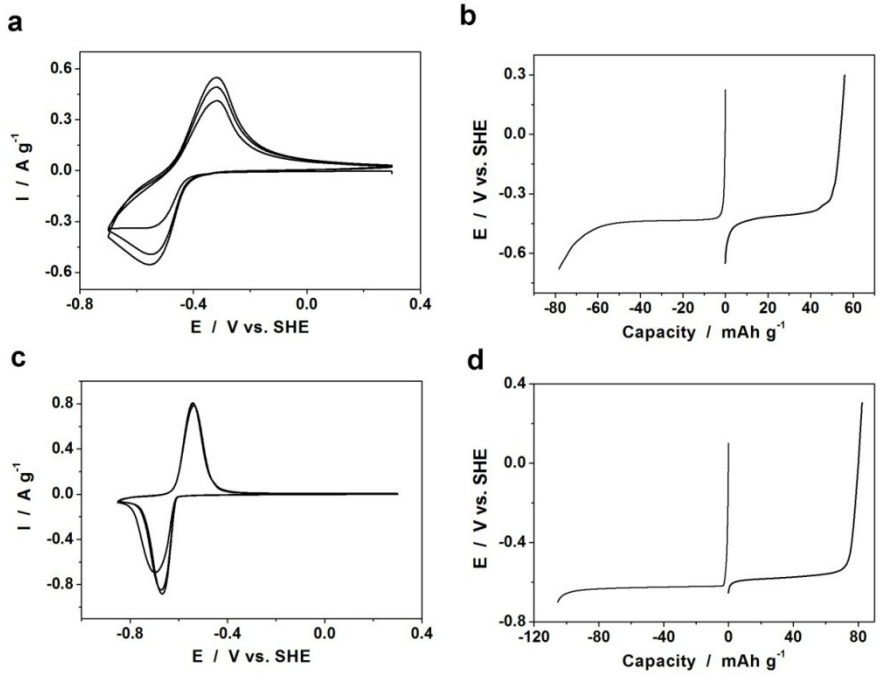

Figure S5. (a, c) Cyclic voltammograms at a scan rate of 0.3 mV s^{-1} for carbon-coated $NaTi_2(PO_4)_3$ in 0.5 M Na_2SO_4 and TiP_2O_7 in 0.5 M Li_2SO_4 (initial 3 cycles). **(b, d)** galvanostatic profiles of carbon-coated $NaTi_2(PO_4)_3$ and TiP_2O_7. All electrode potentials are vs. standard hydrogen electrode (SHE).

Figure S6

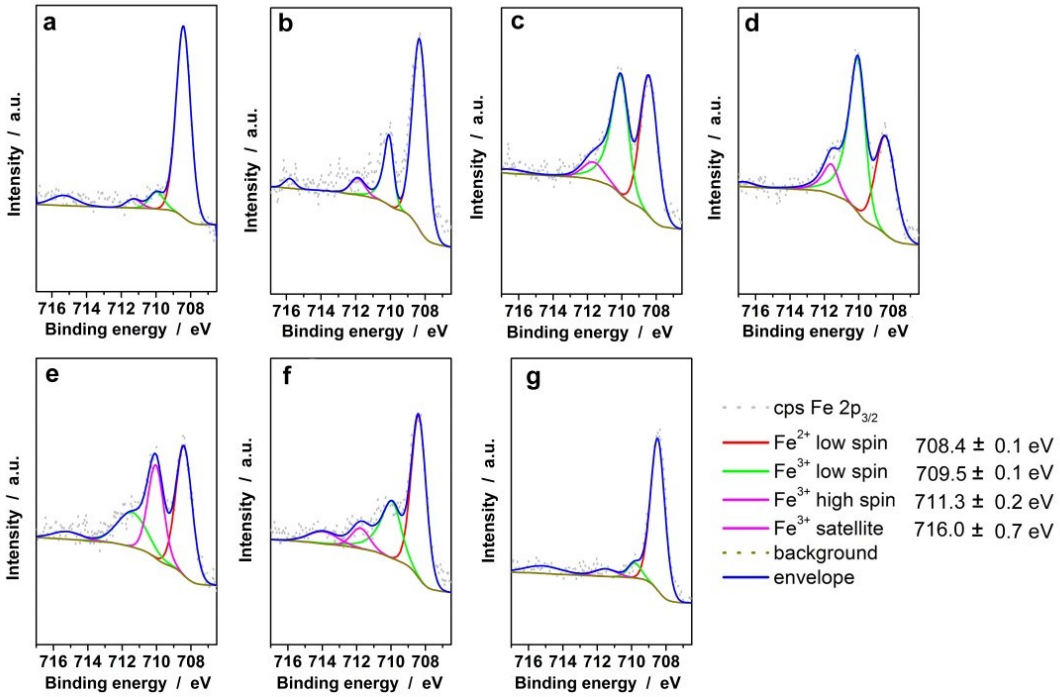

Figure S6 a-g. *ex-situ* XPS peak fitting spectra from Fe $2p_{3/2}$ core level of CuHCF at different charging/discharging states.

Figure S7

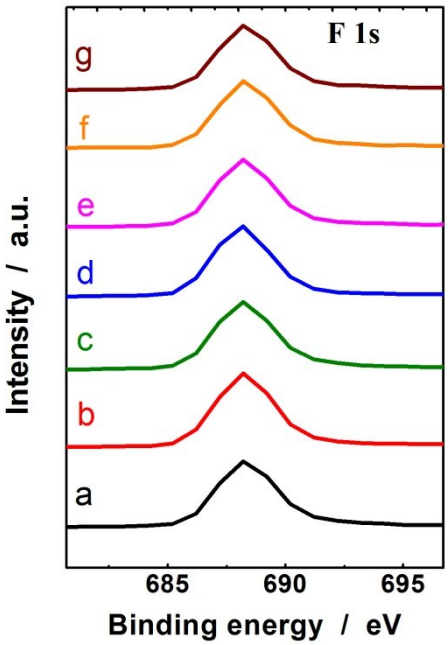

Figure S7. *Ex-situ* XPS spectra recorded from F 1s score level of CuHCF/Gr at a-g states. The explanations of different states are illustrated in the caption of Figure 5 in the manuscript.

Table S1. Structural parameter of CnHCF in the *Fm-3m* structure determined from Rietveld method using powder X-ray diffraction data (Rietveld) and *ab initio* calculations with the GGA+U approximation (GGA+U).

Structural parameters		**Value**	
		Rietveld	***GGA+U***
Lattice parameter	a = b = c	10.09	10.22
	α = β = γ	90°	90°
Bond distance	Fe-C	1.92Å	1.92Å
	Cu-N	1.92Å	2.05Å
	C-N	1.21Å	1.17Å
Angle	∠Cu-N-C	180°	180°
	∠Fe-C-N	180°	180°

Table S2. The compositions of Fe(II) and Fe(III) in CuHCF/Gr at different states via peak fitting of XPS spectra.

States	Percentage / %		
	Fe(II)	Fe(III)	Fe(III)/ Fe(II)
a	84.25	15.75	0.19
b	66.36	33.64	0.51
c	47.45	52.55	1.11
d	40.63	59.37	1.46
e	44.07	55.93	1.27
f	57.52	42.48	0.74
g	81.64	18.36	0.22

Table S3. Atomic concentration of different elements in graphene modified CuHCF during electrochemical cycling.

States	Atomic concentration / %			
	K	Fe	N	Cu
a	5.38	14.21	46.06	8.77
b	3.47	18.33	41.86	10.63
c	2.55	17.39	44.84	10.27
d	0.64	17.74	42.82	12.49
e	2.01	20.21	42.12	10.13
f	2.94	18.64	44.80	10.32
g	5.22	12.01	46.52	11.21

Table S4. Mole ratio of different elements in graphene modified CuHCF during charging process.

States	Mole ratio / %					
	Na/Fe	**K/Fe**	**(Na+K)/Fe**	**Na/Fe**	**K/Fe**	**Na/K**
	0.5M Na_2SO_4	**0.5M K_2SO_4**	**0.1M Na_2SO_4 + 0.4M K_2SO_4**			
Q_1	78.21	92.14	83.85	4.06	79.79	5.09
Q_2	49.12	42.12	39.55	3.32	36.23	9.17
Q_3	4.30	3.46	2.99	0.99	1.99	49.83